Comparison of Passivity Based Controller with Adaptive Passivity Controller for Cascaded converter systems

Avanish Pratap Singh[1, a], Dr. Krishna Singh[1, b], Sanjay Kumar[1, c]

[1] Department of Electronics and Communication Engineering, G.B. Pant DSEU Okhla 1 Campus, Delhi

Abstract— The Passivity Based Controller (PBC) utilizes an energy-based core, making it a reliable and straightforward development option. When a constant power load is present in DC microgrid systems, PBC is used to address instability issues in cascaded converter systems caused by input voltage changes and parametric uncertainty in the dc-dc buck power converter. To improve the control's robustness to variations in both the load and the line, a nonlinear disturbance observer (NDO) is designed and used as a feed-forward channel to compensate for disturbances. The NDO employs a disturbance estimation technique in conjunction with the PBC controller. In cascading converter systems, two buck converters are connected in sequence, with the source power converter being the first buck converter connected to the DC microgrid. A second power converter is connected to the first power converter to create a constant power load (CPL). However, due to CPL's negative resistance characteristic, stability issues arise. Simulation results are presented to illustrate the effectiveness of PBC with NDO when used with cascaded power converters.

Keywords—Constant Power Load (CPL), Non-Linear disturbance Observer (NDO), Passivity Based Controller (PBC), Microgrid, Buck Converter.

I. INTRODUCTION

DC microgrids have proven to be a viable alternative to traditional AC networks because they offer a favorable setting for integrating DC renewable energy sources, DC loads, and energy storage systems [1]. The use of cascaded buck power converters, which include point-of-load converters, enables power conditioning and regulation. The point-of-load converters, which can regulate power, behave similarly to CPL [2]. A typical DC distribution system is shown in Figure 1, where the first converter acts as a line-regulating converter, and a second-stage buck converter with a load act as the CPL.

Upon modeling the system based on its initial concept, it was determined to be a second-order nonlinear system. To create a conventional linear controller such as a PID, the model will need to be linearized around a specific operating point. However, these controls are only effective for small disturbances. To ensure stability under larger disturbances, an intelligent controller using advanced techniques must be developed.

The literature suggests that passivity control strategy is an innovative technology that ensures the robust stability of a DC-DC buck converter[4].
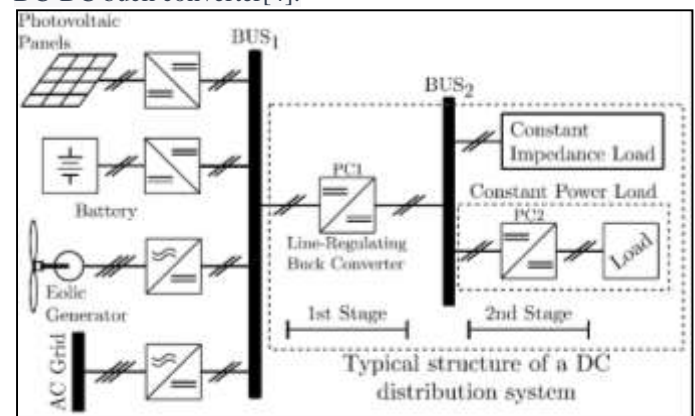

Fig. 1 DC distribution system [3]

Incorporating a nonlinear disturbance observer (NDO) has been shown to enhance the control performance of a DC-DC boost converter supplying a CPL [5]. This control approach delivers global stability even with high CPL variations and rapid dynamic response, surpassing the performance of linear control. By maintaining the system's passive property and incorporating NDO as an amendment to the current PBC method, this technique can swiftly restore and minimize system disturbances and uncertainty.

A. Paper organisation

The system's specifications are discussed in section II. The passivity controller based design is concluded in section III. Section IV of the report shows simulation outcomes for the DC distribution system.

II. SYSTEM DETAILS

The general layout of common dc microgrid systems, Buck converter , constant power load is shown in Fig. 1.

A. *DC Microgrid*

In Figure 1, the primary AC grid, energy storage systems, and various renewable energy sources (e.g., photovoltaic panels, batteries, and eolic generators) are utilized to supply power to the sources bus (Bus 1). Meanwhile, all the loads, including constant impedance load and constant power load, are linked to the load bus (Bus 2).

B. *DC-DC Converter*

As depicted in Figure 1, a buck converter called PC1 is employed to regulate the voltage from Bus 1 to that of Bus 2. This stage, which decreases the voltage, is referred to as the 1st stage. The 2nd stage refers to the point at which all loads are connected. The circuit diagram for the buck converter can be seen in Figure 2.
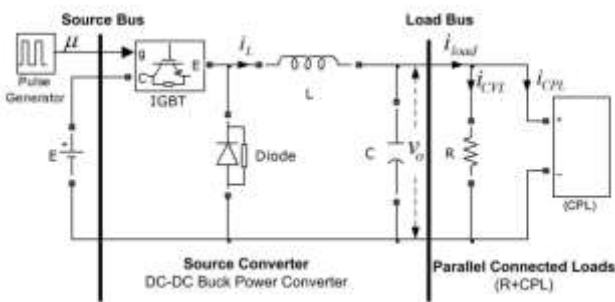

Fig.2 DC-DC Buck Converter [6]

Figure 2 illustrates a conventional cascaded system with parallelly coupled loads (R + CPL) and an open-loop buck power converter. The diagram identifies the circuit's key components, including the capacitor, inductance, load resistance, and input voltage, which are represented by C, L, R, and E, respectively. The inductor current, capacitor voltage, and duty ratio are each represented by the symbols i_L, v_o, and $\mu \in [0, 1]$.

(1) describes the mathematical relationship between the input voltage and the output voltage of a buck converter.

$$\mu = \frac{v_o}{E} \qquad (1)$$

Buck converters can function in either Continuous Conduction Mode (CCM) or Discontinuous Conduction Mode (DCM) based on the inductor current. In CCM, the inductor current of the buck converter never reaches zero, making it the primary focus for controller design in this study.

C. *Constant Power Load*

A Constant Power Load refers to a load that maintains a constant output power level, thereby resulting in the drive system's efficiency being considered 100%. Power converter loads can be considered as CPLs when they are adequately maintained. One way to model CPL is as:

$$i_{cpl} = \frac{P_{cpl}}{v_o} \qquad (2)$$

If ($\Delta v / \Delta i > 0$) the incremental impedance of the CPL will be positive and if ($\Delta v / \Delta i < 0$) the incremental impedance of the CPL will be negative which has a destabilizing impact on DC microgrid systems.
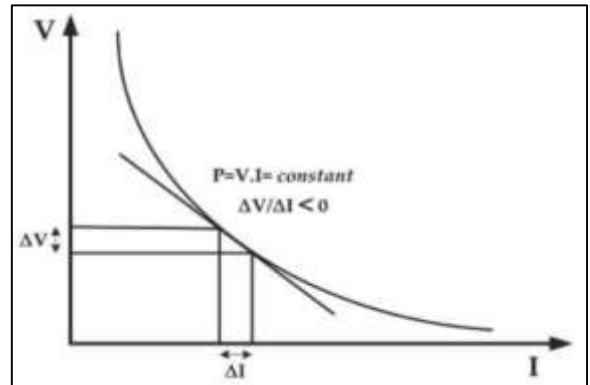

Fig.3 V-I plot of CPL [7]

Fig.4 depicts the whole system under analysis, and [3] includes a mathematical description of the system. Negative incremental impedance negatively affects the operation of multi-stage converter systems with variations in supply voltage, causing uncertainty in system performance [3].
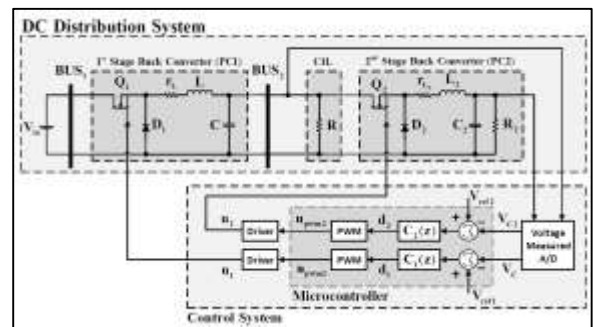

Fig.4 DC Distribution system [3]

If the load resistance R>R_{CPL}, the load bus voltage will start oscillating because the system becomes impassive which means that the energy in the system will start oscillating between the inductor and the capacitor. So, to make it stable we have to make a system as a passive system where the R<R_{CPL} .

III. DESIGN OF CONTROLLER

The following is a description of the DC-DC Buck converter's model structure:

$$\dot{i_L} = \frac{E}{L}\mu - \frac{v_o}{L} \qquad (3)$$

$$\dot{v_0} = \frac{i_L}{C} - \frac{v_o}{CR} - \frac{P}{Cv_o} \qquad (4)$$

Considering that CPL instability is the worst-case scenario, it is assumed that all parasitic elements be ignored because of the way it affects the oscillation of the damping mechanism. (3) and (4) can be solved by adding anticipated disturbances and uncertainty to the provided system as follows:

$$\dot{\iota}_L = \frac{E}{L}\mu - \frac{v_o}{L} + d_1 \tag{5}$$

$$\dot{v}_0 = \frac{i_L}{C} - \frac{v_o}{CR} - \frac{P}{Cv_o} + d_2 \tag{6}$$

d_1 represents the disturbance of the system caused by the change in input voltage E and inductance L variation (5) is regrouped into (7)

$$d_1 = \frac{E}{L}\mu - \frac{E_o}{L_o}\mu + \frac{v_o}{L_o} - \frac{v_o}{L} \tag{7}$$

d_2 represent the disturbance of the system produced by change in load resistance, R and the capacitor C variation, (6) is transformed into (8).

$$d_2 = \frac{i_L}{C} - \frac{i_L}{C_o} + \frac{v_o}{C_o R_o} - \frac{v_o}{CR} + \frac{P_o}{C_o v_o} - \frac{P}{Cv_o} \tag{8}$$

where L_o, C_o, R_o and E_o represents the ideal values of L, C, R and E respectively. Considering the matrices given below, (3)-(6) can be regrouped as in (9) and (10).

$$H\dot{Z} + [G + R(z)]Z = \mu\Gamma \tag{9}$$

$$H_o\dot{Z} + [G + R_o(z)]Z = \mu\Gamma_o + d \tag{10}$$

Where,

$$Z = \begin{pmatrix} z_1 \\ z_2 \end{pmatrix} = \begin{pmatrix} i_L \\ v_o \end{pmatrix}, H = \begin{pmatrix} L & 0 \\ 0 & C \end{pmatrix}, G = \begin{pmatrix} 0 & 1 \\ -1 & 0 \end{pmatrix}$$

$$R(z) = \begin{pmatrix} 0 & 0 \\ 0 & \left(\frac{1}{R} + \frac{P}{z_2^2}\right) \end{pmatrix}, and\ \Gamma = \begin{pmatrix} E \\ 0 \end{pmatrix}.$$

A. Design of a passivity based controller

The converter system becomes passive by dissipating the energy by adding virtual resistance R_{1d} and R_{2d} through a passivity-based controller. This acts as if it has a series resistance to the inductor circuit and a parallel resistance across the capacitor circuit. The two stages described below can help realize the PBC approach's design:

1) Energy Shaping stage: This stage can be accomplished by forming terms of (9) to be $Z = \tilde{Z} + Z_d$, yields in (11).

$$H\dot{\tilde{Z}} + [G + R(z)]\tilde{Z} = \mu\Gamma - (H\dot{Z}_d + [G + R(z)]Z_d) \tag{11}$$

and $\tilde{Z}$ is the magnitude of the deviation from the desired values Z_d. This stage helps in finding the energy stored in inductor and capacitor circuits.

2) Damping Injection stage: This stage can be derived by incorporated the damping injection resistance matrix $R_d\tilde{Z}$ for both sides of (11), to get (12).

$$H\dot{\tilde{Z}} + [G + R_i(z)]\tilde{Z} = \mu\Gamma - (H\dot{z}_d + [G + R(z)] - R_d\tilde{Z}) \tag{12}$$

By defining the resistance matrices as in (13) and (14).

$$R_i(z) = \begin{pmatrix} R_{1d} & 0 \\ 0 & \left(\frac{1}{R_{2d}} + \frac{1}{R} + \frac{P}{z_2^2}\right) \end{pmatrix} \tag{13}$$

$$R_d = R_i(z) - R(z) = \begin{pmatrix} R_{1d} & 0 \\ 0 & \frac{1}{R_{2d}} \end{pmatrix} \tag{14}$$

The system will become entirely passive as a result of the addition of virtual resistances to the converter, which manages the dissipation of transient energy of the converter circuit and is also in accordance with the Lyapunov stability. As a result, the left side of (10) reaches the globally stable equilibrium point $\tilde{Z}= 0$. The stable control strategy can be designed based on (11) as given in (12):

$$\mu\Gamma - (H\dot{Z}_d + [G + R(z)] - R_d\tilde{Z}) = 0 \tag{15}$$

From (12), it is divided in to (16) and (17).

$$\mu E - L\dot{z}_{1d} - z_{2d} + R_{1d}(z_1 - z_{1d}) = 0 \tag{16}$$

$$-C\dot{z}_{2d} + z_{1d} - \frac{z_{2d}}{R} - \frac{P}{z_{2d}} + \frac{1}{R_{2d}}(z_2 - z_{2d}) = 0 \tag{17}$$

(16) and (17) shows the dynamic behavior of controller, which comprises of three degrees of freedom (μ, z_{1d}, z_{2d}). It can be seen that only two loops are needed to find the required control signal μ.

The output voltage regulation is done by substituting $z_{2d} = V_o$, and $\dot{z}_{2d}$ is equal to zero and $z_{1d} = I_L$, and thus, $\dot{z}_{1d}$ is equal to zero. Finally, (16) and (17) are converted into to (18) and (19) as given below:

$$\mu E - V_o + R_{1d}(i_l - I_L) = 0 \tag{18}$$

$$I_L - \frac{V_o}{R} - \frac{P}{V_o} + \frac{1}{R_{2d}}(v_o - V_o) = 0 \tag{19}$$

The inner inductor current feedback loop and the output voltage outer loop serve as the foundation for the control signal. Based on the output voltage feedback error, the outer voltage loop control adjusts the reference inductor current I_L.

(4) is rearranged as in (20) given below,

$$i_L = C\dot{v}_0 + \frac{v_o}{R} + \frac{P}{v_o} \tag{20}$$

By Substituting (19) and (20) in (18), (21) can be derived below:

$$\mu = \frac{1}{E}\left[-R_{1d}C\dot{v}_0 + R_{1d}\left(\frac{1}{R} + \frac{1}{R_{2d}}\right)(V_o - v_o) + V_o\right] \tag{21}$$

By considering error signal $\tilde{Z} = V_o - v_o$, PBC controller can be derived by (22),

$$\mu = k_d\dot{\tilde{Z}} + k_p\tilde{Z} + D \tag{22}$$

where k_p and k_d are the proportional and derivative gains respectively are given below,

$$k_d = \frac{R_{1d}C}{E}, k_p = \frac{R_{1d}}{E}\left(\frac{1}{R} + \frac{1}{R_{2d}}\right), and\ D = \frac{V_o}{E}.$$

A simple solution is required to resolve the problem. By changing (18), and then adjusting for the amount of disturbances ("d"), or the deviation in the inductor current and capacitor voltage caused by changes in load or input voltage. Equation (18) transforms into

$$\mu E - V_o + R_{1d}(i_l - I_L) + d1 = 0 \qquad (23)$$

$$I_L - \frac{V_o}{R} - \frac{P}{V_o} + \frac{1}{R_{2d}}(v_o - V_o) + d2 = 0 \qquad (24)$$

This amount of disturbance can be added to the existing closed-loop controller (PBC) through the feed-forward channel to minimize the steady-state output voltage inaccuracy brought on by load and line changes. Therefore, (23) and (24) becomes

$$\mu = \frac{1}{E}(V_o + R_{1d}(I_L - i_l) - d1 \qquad (25)$$

$$I_L = \frac{V_o}{R} + \frac{P}{V_o} + \frac{1}{R_{2d}}(V_o - v_o) - d2 \qquad (26)$$

B. Design of a Adaptive passivity based controller

The disturbances in (25), which are time-varying and irrational signals, depend on the system's operational states. In this specific instance, both the CPL variation itself and the change brought on by the fluctuation of output voltage v_o are affected by the disturbances of the current drown caused by the CPL. Through the NDO, this estimates these disturbances appropriately. The estimated values $\hat{d} = [\hat{d}_1 \ \hat{d}_2]^T$

$$\begin{pmatrix} \dot{i}_l \\ \dot{v}_o \end{pmatrix} = \underbrace{\begin{pmatrix} -\frac{v_o}{L} \\ \frac{i_l}{C_o} - \frac{v_o}{C_o R_o} - \frac{P_o}{C_o v_o} \end{pmatrix}}_{f(z)} + \underbrace{\begin{pmatrix} \frac{E_o}{L_o} \\ 0 \end{pmatrix}}_{g_1(z)} \mu + \underbrace{\begin{pmatrix} 1 & 0 \\ 0 & 1 \end{pmatrix}}_{g_2(z)} d \quad (27)$$

$$\underbrace{\phantom{\begin{pmatrix} \dot{i}_l \\ \dot{v}_o \end{pmatrix}}}_{\dot{z}}$$

therefore (27) conforms to the following system form.

$$\dot{z} = f(z) + g_1(z) * \mu + g_2(z) * d \qquad (28)$$

$$y_o = h(z)$$

where y_o is the system's output. The following fundamental NDO can be used to estimate the unknown disturbance "d" as

$$\dot{\hat{d}} = \ell(z) [\dot{z} - f(z) - g_1(z) * \mu - g_2(z) * \hat{d} \ ] \qquad (29)$$

where $\ell(z)$ stands for the nonlinear gain of the observer. The derivative of the state z makes it difficult to implement the disturbance observer in (29) It is essential to define the value of an auxiliary variable as a result.

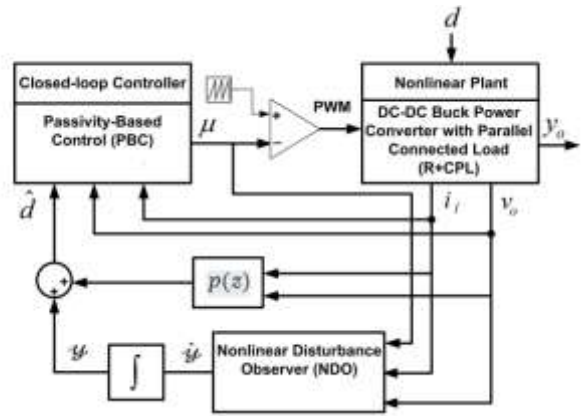$$y = \hat{d} - \rho(z) \qquad (30)$$

Fig.5 The nonlinear plant with the composite feedback controller (PBC with NDO).[6]

where $\ell(z)$ is the nonlinear function vector that needs to be created and $y \in R^l$ is the internal state of the nonlinear observer. When $\ell(z) = (d\rho(z)/dz)$, the nonlinear disturbance gain $\ell(z)$ is calculated. And

$$\dot{y} = \dot{\hat{d}} - \frac{d\rho(z)}{d(z)} \dot{z} \qquad (31)$$

Consequently, by invoking (27), (28), (29) and (30) with (31), the NDO will become

$$\dot{y} = - \ell(z)y - \ell(z) [f(z) + g_1(z) * \mu + g_2(z) * \rho(z)]$$

$$\hat{d} = y + \rho(z) \qquad (32)$$

Fig.5 depicts the general arrangement of the nonlinear plant with the composite nonlinear controller (NDO with PBC). For stability check-up purposes, the dynamics of the estimation error brought on by disturbances are maintained by

$$\dot{e}_d = \dot{\hat{d}} - \dot{d} = \dot{y} + \frac{d\rho(z)}{d(z)} \dot{z} \qquad (33)$$

By substituting (27) and (32) in (33), yields

$$\dot{e}_d = - \ell(z)(\hat{d} - d) = - \ell(z)e_d \qquad (34)$$

Given that (34) is asymptotically stable, it follows that the disturbance estimation error will converge to zero regardless of the observer gain value chosen, $\ell(z)$. The observer gain can therefore be expressed in the following way:

$$\ell(z) = \begin{pmatrix} \lambda_1 & 0 \\ 0 & \lambda_2 \end{pmatrix} \text{ and thus } p(z) = \begin{pmatrix} \lambda_1 i_l \\ \lambda_2 v_o \end{pmatrix}$$

Finally (32) becomes

$$\begin{cases} \dot{y}_1 = - \lambda_1 y_1 + \lambda_1 [-\frac{E_o}{L_o}\mu + \frac{v_o}{L_o} - \lambda_1 i_l] & (35) \\[2mm] \widehat{d_1} = y_1 + \lambda_1 i_l \end{cases}$$

$$\begin{cases} \dot{y}_2 = - \lambda_2 y_2 + \lambda_2 [\frac{v_o}{C_o R_o} - \frac{i_l}{C_o} + \frac{P_o}{C_o v_o} - \lambda_2 v_o] & (36) \\[2mm] \widehat{d_2} = y_2 + \lambda_2 v_o \end{cases}$$

In order to implement the final control strategy, the amount of plant disturbances d_1 and d_2 in (25) and (26), by their estimated values $\widehat{d_1}$ and $\widehat{d_2}$ as follows:

$$\mu = \frac{1}{E}(V_o + R_{1d}(I_L - i_l) - \widehat{d_1}) \qquad (37)$$

$$I_L = \frac{V_o}{R} + \frac{P}{V_o} + \frac{1}{R_{2d}}(V_o - v_o) - \widehat{d_2}$$

IV. SIMULATION RESULTS

In this section, simulations of Figure.4 steady state and transient states at various supply voltages and parameter values are shown. Table I lists the specifications of cascaded converters. Table II lists the input voltage range and parameter change.

Table I. CONVERTER SPECIFICATIONS [3]

Symbol	Parameter	Value
	Line regulating Buck Converter(PC1)	
E	$Microgrid(BUS1)\ Voltage$	50 V
V_o	$PC1\ Output(BUS2)\ Voltage$	24 V
	CPL Buck Converter(PC2)	
E_1	$PC2\ Input(BUS_2)\ Voltage$	24 V
V_{o2}	CPL Output Voltage	15 V
$L\ and\ L_2$	Inductor Inductance	2.5 mH
$C\ and\ C_2$	Capacitors	2200 μF

Table II. MINIMUM AND MAXIMUM LIMITS OF INPUT VOLTAGE AND PARAMETER VALUES [3]

Symbol	Nominal Values	Minimum limit Values	Maximum limit Values
E	50 V	40 V	60 V
r_L, r_{L2}	50 mΩ	48.5 mΩ	52.5 mΩ
R	10 Ω	5 Ω	15 Ω
R_2	5 Ω	2.5 Ω	7.5 Ω

In order to evaluate the disturbance rejection and quick recovery capabilities of the PBC and PBC+I controllers, simulations were performed. Virtual resistance values of $R_{1d} = 5 * 10^5$ and $R_{2d} = 500$ were chosen for PBC based on energy dissipation in the inductor circuit and capacitor, respectively. Virtual series resistance R_{1d} should be sufficiently strong to ensure a vast amount of energy dissipation in the inductor circuit and good ripple reduction.

This is the major goal behind the selection of the values of R_{1d} and R_{2d}. The parallel virtual resistance R_{2d}, which will be utilized to reduce ripples in the capacitor circuit, should also be set at a low value.

Figure 6 displays the system's response to changes in supply voltage and parameter settings for the passivity-based controller.

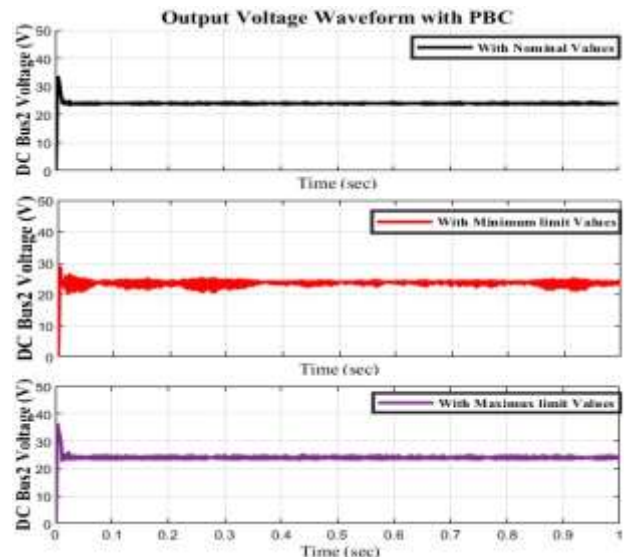*(a) Simulation of Cascaded DC-DC Power Buck converters with PBC:*

Fig.6. BUS2 voltage (Source Converter) output waveforms with parameter and input voltage variations with PBC.
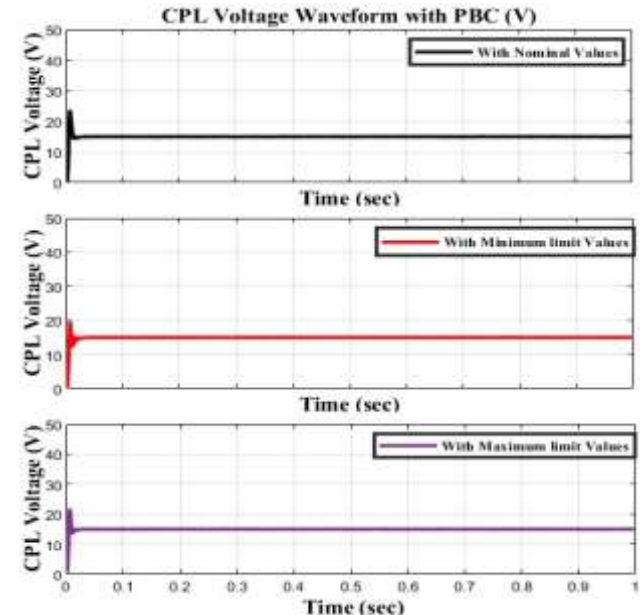

Fig.7 Point-of-Load converter (CPL) output voltage waveform with parameter and input voltage variations with PBC

The output voltage waveforms of the source converter (BUS2) and point-of-load converter (CPL) initially exhibit transient overshoot and eventually settle at steady-state values of 24V and 15V, respectively. However, when exposed to input voltage and parameter fluctuations, the output voltage waveform of the source converter displays

minor ripples in the steady state, while the output voltage waveform of the point-of-load converter shows no steady-state error but with slight undershoot.

(b) *Simulation of Cascaded DC-DC Power Buck converters with Adaptive PBC:*
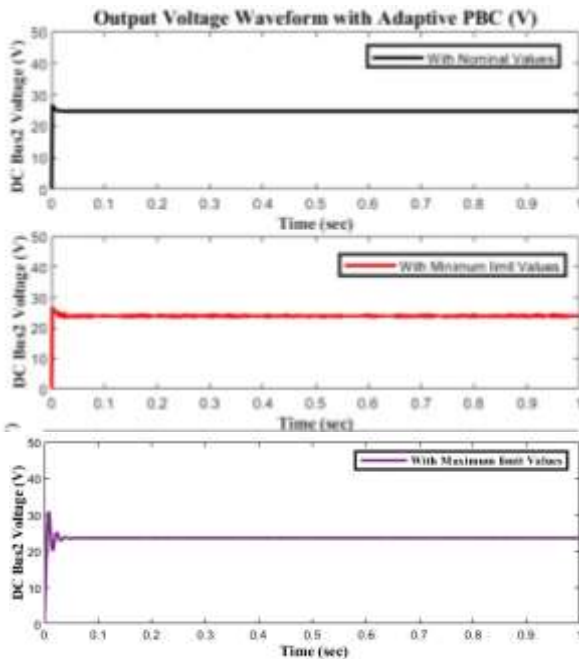

Fig.8 BUS2 voltage (Source Converter) output waveforms with parameter and input voltage variations with Adaptive PBC.
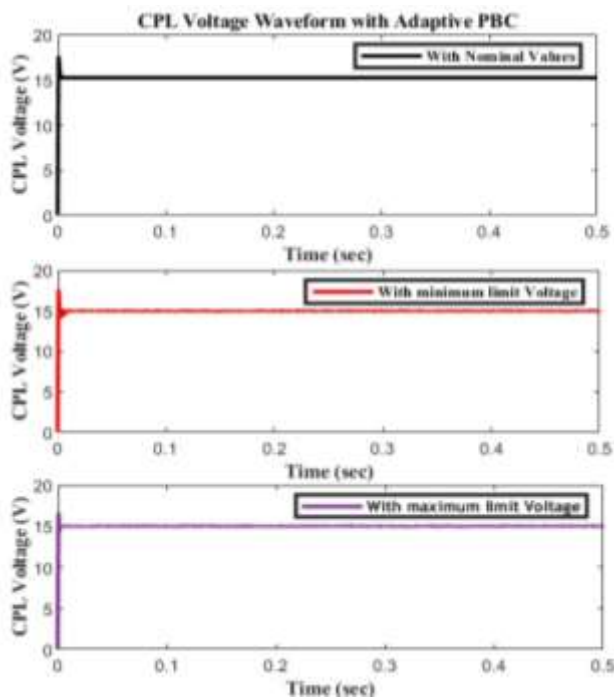

Fig.9 Point-of-Load converter (CPL) output voltage waveform with parameter and input voltage variations with Adaptive PBC.

The results indicate that the Adaptive PBC has decreased the overshoot in comparison to the PBC. The output voltage waveform of the source converter (BUS2) exhibits reduced ripples for the minimum and maximum limit values, and the output voltage waveform of the Point-of-Load converter (CPL) displays zero steady-state error.

V. CONCLUSION

The purpose of this study is to compare the performance of Passivity Based Controller (PBC) and Adaptive PBC in cascaded power converters (two stages) to enhance microgrid performance. Simulation results indicate that Adaptive PBC outperforms PBC in handling various disturbances. The future scope of the study includes the implementation of Adaptive PBC on a DC-DC converter system to obtain hardware results, which will be presented in a future paper.

VI. REFERENCES

[1] Y. Ito, Y. Zhongqing, and H. Akagi, "DC microgrid based distribution power generation system," in Proc. 4th Int. Conf. Power Electron. Motion Control (IPEMC), Aug. 2004, pp. 1740–1745.

[2] Su, Mei, Zhangjie Liu, Yao Sun, Hua Han, and Xiaochao Hou. "Stability analysis and stabilization methods of DC microgrid with multiple parallel-connected DC–DC converters loaded by CPLs." *IEEE Transactions on Smart Grid* 9, no. 1 (2016): 132-142.

[3] Lucas, K.E., Pagano, D.J., Vaca-Benavides, D.A., Garcia-Arcos, R., Rocha, E.M., Medeiros, R.L. and Rios, S.J., 2020. "Robust Control of Interconnected Power Electronic Converters to Enhance Performance in dc distribution systems: A case of study. " *IEEE Transactions on Power Electronics*, 36(4), pp.4851-4863.

[4] W. J. Gil-González, O. D. Montoya, A. Garces, F. M. Serra and G. Magaldi, "Output Voltage Regulation For dc–dc Buck Converters: a Passivity–Based PI Design," *2019 IEEE 10th Latin American Symposium on Circuits & Systems (LASCAS)*, Armenia, Colombia, 2019,pp.189-192,doi: 10.1109/LASCAS.2019.8667557.

[5] Q. Xu, C. Zhang, C. Wen, and P. Wang, "A novel composite nonlinear controller for stabilization of constant power load in DC microgrid," IEEE Trans. Smart Grid, vol. 3053, p. 1, 2017.

[6] Hassan, Mustafa Alrayah, et al. "Adaptive passivity-based control of DC– DC buck power converter with constant power load in DC microgrid systems." *IEEE Journal of Emerging and Selected Topics in Power Electronics* 7.3 (2018): 2029- 2040.

[7] Al-Nussairi, Mohammed Kh, Ramazan Bayindir, and Eklas Hossain. "Fuzzy logic controller for Dc-Dc buck converter with constant power load." In *2017 IEEE 6th International Conference on Renewable Energy Research and Applications (ICRERA)*, pp. 1175-1179. IEEE, 2017.

[8] Q. Xu, C. Zhang, C. Wen, and P. Wang, "A novel composite nonlinear controller for stabilization of constant power load in DC microgrid," IEEE Trans. Smart Grid, vol. 3053, p. 1, 2017.